NeuroImage 258 (2022) 119337

Contents lists available at ScienceDirect

NeuroImage

journal homepage: www.elsevier.com/locate/neuroimage

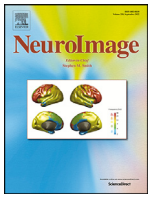

Eyes-closed versus eyes-open differences in spontaneous neural dynamics during development

Nathan M. Petro[a], Lauren R. Ott[a], Samantha H. Penhale[a], Maggie P. Rempe[a,b], Christine M. Embury[a,c], Giorgia Picci[a], Yu-Ping Wang[d], Julia M. Stephen[e], Vince D. Calhoun[e,f], Tony W. Wilson[a,g,*]

[a] Boys Town National Research Hospital, Institute for Human Neuroscience, 378 Bucher Circle, Boys Town, NE 68010, USA
[b] College of Medicine, University of Nebraska Medical Center, Omaha, NE, USA
[c] Department of Psychology, University of Nebraska Omaha, Omaha, NE, USA
[d] Department of Biomedical Engineering, Tulane University, New Orleans, LA, USA
[e] Mind Research Network, Albuquerque, NM, USA
[f] Tri-Institutional Center for Translational Research in Neuroimaging and Data Science (TReNDS), Georgia State University, Georgia Institute of Technology, and Emory University, Atlanta, GA, USA
[g] Department of Pharmacology & Neuroscience, Creighton University, Omaha, NE, USA

ARTICLE INFO

Keywords:
Magnetoencephalography
MEG
Oscillations
Resting state
Beta
Alpha
Adolescence

ABSTRACT

Background: Assessing brain activity during rest has become a widely used approach in developmental neuroscience. Extant literature has measured resting brain activity both during eyes-open and eyes-closed conditions, but the difference between these conditions has not yet been well characterized. Studies, limited to fMRI and EEG, have suggested that eyes-open versus -closed conditions may differentially impact neural activity, especially in visual cortices.

Methods: Spontaneous cortical activity was recorded using MEG from 108 typically developing youth (9-15 years-old; 55 female) during separate sessions of eyes-open and eyes-closed rest. MEG source images were computed, and the strength of spontaneous neural activity was estimated in the canonical delta, theta, alpha, beta, and gamma bands, respectively. Power spectral density maps for eyes-open were subtracted from eyes-closed rest, and then submitted to vertex-wise regression models to identify spatially specific differences between conditions and as a function of age and sex.

Results: Relative alpha power was weaker in the eyes-open compared to -closed condition, but otherwise eyes-open was stronger in all frequency bands, with differences concentrated in the occipital cortex. Relative theta power became stronger in the eyes-open compared to the eyes-closed condition with increasing age in frontal cortex. No differences were observed between males and females.

Conclusions: The differences in relative power from eyes-closed to -open conditions are consistent with changes observed in task-based visual sensory responses. Age differences occurred in relatively late developing frontal regions, consistent with canonical attention regions, suggesting that these differences could be reflective of developmental changes in attention processes during puberty. Taken together, resting-state paradigms using eyes-open versus -closed produce distinct results and, in fact, can help pinpoint sensory related brain activity.

1. Introduction

Brain activity during periods of rest – in which participants are relaxed and not engaged in an explicit cognitive task (Azeez and Biswal, 2017; Biswal et al., 1995; Fox and Raichle, 2007) – has received considerable attention in human neuroimaging research. The absence of task demands makes this method useful to generalize across samples. Further, it is particularly applicable to developmental populations and those with severe psychiatric and neurological conditions, where cognitive/linguistic abilities may affect performance on cognitive tasks during imaging and thereby complicate interpretation. In this regard, resting state studies have made progress toward identifying brain networks that undergo considerable changes during development (Marusak et al., 2017; Uddin et al., 2011), which have shed light on how developmental differences may underlie the emergence of psychiatric disorders (Drysdale et al., 2017; van Dijk et al., 2010).

* Corresponding author at: Boys Town National Research Hospital, Institute for Human Neuroscience, 378 Bucher Circle, Boys Town, NE 68010, USA.
E-mail address: tony.wilson@boystown.org (T.W. Wilson).

https://doi.org/10.1016/j.neuroimage.2022.119337.
Received 6 January 2022; Received in revised form 24 May 2022; Accepted 26 May 2022
Available online 27 May 2022.

While the majority of resting state studies in developing youth have focused on functional connectivity as recorded in the blood-oxygenation-level dependent (BOLD) signal, there is growing interest in the use of magnetoencephalography (MEG) to measure spontaneous brain activity. Distinct advantages of MEG in this context are that the neuromagnetic field strength estimates are reference free (e.g., in contrast to electrical referencing in electroencephalography; EEG), and do not require a contrast condition of any type (e.g., in fMRI). Further, MEG possesses exquisite spatial (~3–5 mm; Baillet, 2017; Wilson et al., 2016) and temporal (1 ms) precision, which enables a multispectral approach whereby neural activity at different frequencies can be quantified and characterized discretely. Importantly, MEG is noninvasive and silent, making it ideal for the assessment of resting brain activity in developing youth (Hoshi and Shigihara, 2020; Ott et al., 2021), who may be particularly sensitive to the noise and restricted environment of MRI data collection.

To date, age-related differences in spontaneous cortical activity, as measured by M/EEG, are somewhat limited though generally consistent. Multiple studies have documented that, across the entire lifespan, younger compared to older subjects tend to show stronger oscillatory power in lower frequency bands and weaker power in the higher frequency bands, as measured by both EEG (Michels et al., 2013; Segalowitz et al., 2010) and MEG (Gómez et al., 2013; Hoshi and Shigihara, 2020; Hunt et al., 2019; Uhlhaas et al., 2010). A recent study using MEG observed this age-related effect specifically within a peri-adolescent age range (Ott et al., 2021). Consistent with previous work, this study also demonstrated that these changes occur predominantly in association cortices which show robust structural changes during the pubertal transition period in particular (Gogtay et al., 2004; Wierenga et al., 2014) relative to low-level sensory regions. Albeit limited, this work suggests that developmental differences in resting oscillatory power may reflect important markers of brain development.

A key parameter that has not been examined in developmental studies of resting spontaneous cortical activity is the effect of using eyes-open (EO) versus eyes-closed (EC) recording paradigms. This consideration is particularly important given that at least some frequency bands are sensitive to EO relative to EC conditions vis-à-vis their relationship to sensory processes. Most notably, posterior alpha power shows a well-documented decrease in power following the opening of the eyes (Berger, 1929; Cohen, 1968), an effect which reflects visual cortical processing of external sensory information (Pfurtscheller, 1992). Similar changes, when the eyes are open, are found during states of heightened arousal (Barry et al., 2005) and with directed visual attention (Adrian, 1944; Ergenoglu et al., 2004), demonstrating that occipital alpha power is intimately tied to visual processing encompassing both low-level visual sensory processes and higher-level processes such as attention (Klimesch et al., 2007). Indeed, a few studies that have directly compared resting cortical activity between these conditions have found a decrease in alpha power for EO relative to EC (Allen et al., 2018; Barry et al., 2007, 2009;). Along these lines, other studies have demonstrated that functional connectivity within the visual cortex changes between EO and EC conditions (Agcaoglu et al., 2020; Patriat et al., 2013). Thus, the existing evidence indicates that there may be important differences between resting-state activity in EO and EC conditions, and that these may be related to both low-level sensory processing and higher-order attention function.

In the current cross-sectional study, spontaneous cortical activity was measured using MEG in a peri-adolescent sample (9-15 years) during periods of EC and EO rest. We expected that conditional differences between EC and EO would be observed primarily in brain areas involved in visual sensory processing. In addition, we tested whether differences in cortical activity between EC and EO were related to age. Here, we hypothesized that conditional differences would be observed in areas involved in higher order sensory processing, such as those within the canonical frontoparietal attention network, given that the structure and function of these regions take shape during pubertal development (Segalowitz et al., 2010). Lastly, we examined if differences in EC versus EO varied between males and females, given the well-documented sexual divergence that emerges specifically during adolescence (Goddings et al., 2019; Mills and Tamnes, 2014).

2. Methods

2.1. Participants

A total of 127 heathy youth (61 Male, 119 right-handed) were enrolled to participate in the study (M_{age} = 11.78 years, SD = 1.60, range = 9.03–15.20 years). A parent or legal guardian provided informed consent and reported all demographic information. The child participants provided assent before participating in the study. The study was fully approved by our Institutional Review Board, and all protocols were conducted in accordance with the Declaration of Helsinki.

Exclusionary criteria included the inability to complete either of the full resting state scans, any medical illness or medication affecting the CNS function, neurological or psychiatric disorders, history of head trauma, current substance abuse, and the standard exclusion criteria related to MEG and MRI acquisition (e.g., dental braces, metallic implants, battery operated implants, and/or any type of ferromagnetic implanted material).

2.2. MEG acquisition

The MEG signals were recorded from a 306-sensor Elekta/MEGIN MEG system (Helsinki, Finland), equipped with 204 planar gradiometers and 102 magnetometers, which sampled the neuromagnetic responses continuously at 1 kHz with an acquisition bandwidth of 0.1–330 Hz. Recordings took place inside a one-layer magnetically-shielded room with active shielding engaged for environmental noise compensation. Participants were seated in a custom-made nonmagnetic chair, with their heads positioned within the sensor array.

Participants were instructed to either rest with their eyes closed or open while fixating on a centrally presented cross during two separate six-minute blocks; the order of the blocks (i.e., EO and EC conditions) was counter-balanced across participants. Participants were monitored throughout MEG data acquisition via live audio-video feeds inside the shielded room. Structural T1 weighted images were acquired on a Siemens 3T Skyra scanner with a 32-channel head coil and using a MPRAGE sequence (TR = 2400 ms; TE = 1.94 ms; flip angle = 8°; FOV = 256 mm; slice thickness = 1 mm (no gap); base resolution = 256; 192 slices; voxel size = 1 × 1 × 1 mm).

2.3. Structural MRI processing and MEG-MRI co-registration

Participants' high-resolution T1-weighted structural MRI data were segmented using a standard voxel-based morphometry pipeline in the computational anatomy toolbox (CAT12 v12.7; Gaser and Dahnke, 2016) within SPM12. Segmented T1 images underwent noise reduction using a spatially-adaptive non-local means denoising filter (Manjón et al., 2010) and a classical Markov Random Field approach (Rajapakse et al., 1997). An affine registration and a local intensity transformation were then applied to the bias corrected images. These preprocessed images were segmented based on an adaptive maximum *a posteriori* technique (Ashburner and Friston, 2005) and a partial volume estimation with a simplified mixed model of a maximum of two tissue types. Lastly, the segmented images were normalized to MNI template space and imported into Brainstorm for co-registration.

Prior to MEG acquisition, four coils were attached to the participants' heads and localized with the three fiducial points and scalp surface using a 3-D digitizer (Fastrak 3SF0002, Polhemus Navigator Sciences, Colchester, VT, USA). After the participant was positioned for MEG recording, an electrical current with a unique frequency label (e.g., 322 Hz) was fed into each of the coils, which induced a measurable magnetic field

and allowed each coil to be uniquely localized relative to the sensors throughout the recording session. Here, because the coil locations were also known in head coordinates, all MEG measurements could be transformed into a common coordinate system. This coordinate system was then used to co-register each participant's MEG data to their structural MRI, prior to source space analyses using Brainstorm (see Section 2.5)

2.4. MEG data pre-processing

Only the gradiometer sensors were used in each stage of MEG preprocessing and analysis. Each MEG dataset was individually corrected for head motion and subjected to noise reduction using the signal space separation method with temporal extension (tSSS; MaxFilter v 2.2; correlation limit: 0.950; correlation window duration: 6 s; Taulu and Simola, 2006). The preprocessing of MEG data was conducted in Brainstorm (Tadel et al., 2019) and was modeled after that of previous studies (Niso et al., 2019; Ott et al., 2021). A high pass filter of 0.3 Hz and notch filters at 60 Hz and its harmonics were applied. Cardiac artifacts were identified in the raw MEG data and removed using an adaptive signal-space projection (SSP) approach, which was subsequently accounted for during source reconstruction (Ille et al., 2002; Uusitalo and Ilmoniemi, 1997). For data collected during the EO session, eye-blink artifacts were additionally removed using the SSP approach. Following artifact removal, data were divided into four-second epochs, which were examined for artifacts on a per-person basis. We opted to use this method to reject other types of artifactual data, as opposed to additional SSP artifact *correction* procedure, to reduce the risk of removing genuine neural information from the signal prior to source reconstruction. Along these lines, we avoided the use of independent components analysis (ICA) to remove artifactual signals, as this would further reduce the rank of the data and thus diminish the precision of source reconstruction. Epochs with amplitudes and/or gradients exceeding ± 3 standard deviations of that individual's distribution of values were excluded from further analysis. Here, individual thresholds, based on the signal distribution for both amplitude and gradient were used to reject artifacts, given that the MEG signal amplitude is strongly affected by the distance between the brain and MEG sensor array. Following this artifact rejection step, the mean number of accepted epochs was 56.55 (SD = 7.69, min = 40, max = 75) for the EO and 65.41 (SD = 6.90, min = 46, max = 89) for the EC conditions. Since the number of epochs can affect the signal-to-noise ratio, we equated the two conditions in each participant by randomly discarding epochs. Thus, participants contributed an average of 55.82 epochs (SD = 6.89, min = 40, max = 71) per condition for analysis. Note that the minimum length of MEG data submitted to the analysis was 160 s (i.e., 40 epochs), which exceeds the minimum recording length recommended to achieve reliable resting state measures (Wiesman et al., 2022). Across participants, the number of epochs were not statistically different by age or sex.

2.5. MEG source imaging and frequency power maps

Source modeling followed the analysis pipeline outlined in Wiesman et al. (2021). Briefly, the forward model was computed using an overlapping spheres head model (Huang et al., 1999), unconstrained to the cortical surface. A linearly constrained minimum variance (LCMV) beamformer, implemented in Brainstorm, was then used to spatially filter the data epochs based on the data covariance, computed from the resting-state recording. Here, we estimated a model with 15,002 vertices across the cortical surface and did not regularize the data covariance matrix.

Using these source estimates, we then computed the power of cortical activity in five canonical frequency bands: delta (2–4 Hz), theta (5–7 Hz), alpha (8–12 Hz), beta (15–29 Hz), and gamma (30–59 Hz). Power spectrum densities (PSD) were estimated using Welch's method (Welch, 1967) on each four-second epoch, with one second sliding Hamming windows overlapping at 50%. The PSDs were then normalized within each frequency band to the total power across the total frequency spectrum per condition, consistent with previous reports on resting state MEG data (Candelaria-Cook et al., 2022; Lew et al., 2021; Niso et al., 2019; Ott et al., 2021; Wiesman et al., 2021, 2022). The PSD maps were then averaged within each participant, separated by the two conditions, and for each of the five frequency bands separately, resulting in 10 PSD maps for each participant. Each of these maps were then projected onto the MNI ICBM152 brain template (Fonov et al., 2009) and a 3 mm FWHM smoothing kernel was applied, before undergoing statistical analysis.

2.6. Statistical analyses

SPM12 was used to assess conditional differences between EC and EO per spectral range in the spontaneous neural dynamics, and to determine if these differences were related to age or sex. To this end, at each vertex and separately for each frequency band, the spontaneous power during EO was subtracted from the EC condition. The difference maps were then submitted to a multiple regression, separately for each frequency band, with the following predictors: (1) a constant term, (2) age, and (3) sex, which represented, respectively, (1) the difference between rest conditions while controlling for age and sex, (2) the relationship between the resting condition difference and age while controlling for sex, and (3) the relationship between the resting condition difference and sex while controlling for age. The coefficient corresponding to each of these three predictors were then submitted to separate F-tests across participants, producing a cortical map possessing vertex-wise F-values. To correct for the multiple comparisons conducted across the vertices, threshold free cluster enhancement (TFCE; E = 1, H = 2; 5000 permutations; Smith and Nichols, 2009) was applied to each of the resulting statistical maps. Following permutations, these TFCE maps were assessed with a cluster-wise threshold of $p_{FWE} < .05$ and a cluster forming threshold of $k > 100$ vertices. Data from the peak voxels were used to display and interpret the corresponding effects, which were labeled with the Harvard-Oxford cortical atlas.

3. Results

3.1. Descriptive statistics

Of the 127 enrolled participants, 9 failed to complete the MRI and 10 failed to complete at least some portion of the MEG resting-state tasks. Thus, the current study included the analysis of data from 108 participants (M_{age} = 11.91, SD = 1.61, range = 9.03–15.20 years). Demographic characteristics are detailed in Table 1.

3.2. Eyes-open versus - closed resting oscillatory activity

The EC compared to EO difference in relative power was assessed using a regression model, which controlled for age and sex. Across all participants, differences in spontaneous neural dynamics between EC and EO resting conditions were found in delta, theta, alpha, beta, and gamma frequency bands. The alpha-band was the only band to show stronger power for EC relative to EO (Fig. 1). This difference was observed in two bilateral clusters, which spanned the occipital, parietal, and temporal cortices, extending into the medial prefrontal cortices; the peak difference was located in the right ($F_{1, 105}$ = 94.63, $p < 0.001$) occipital pole.

Stronger power for EO relative to EC was observed in the delta, theta, beta, and gamma frequency bands. In the delta-band (Fig. 2), this difference was observed in two relatively circumscribed occipital clusters, as well as two bilateral clusters spanning frontal and anterior temporal cortices, with a peak difference located in the right occipital fusiform gyrus ($F_{1, 105}$ = 57.77, $p < .001$). In the theta-band (Fig. 2), this difference was observed in two bilateral clusters spanning the occipital, parietal, temporal, and frontal lobes, with the peak difference located in the right

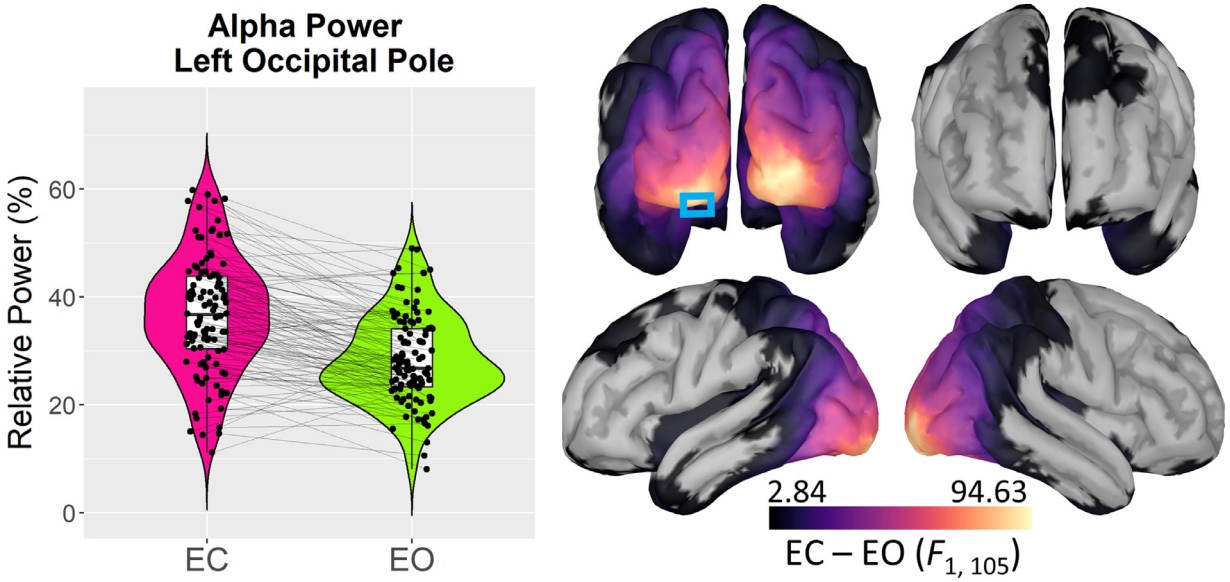

Fig. 1. Resting-state spontaneous alpha differences in EC relative to EO. Cortical surface maps (right) display the vertex-wise F-values representing the comparison of EC to EO relative alpha power passing a TFCE threshold, with the blue box indicating the vertex containing the largest difference. The boxplots are for illustration purposes only and depict the vertex showing the strongest condition effect following multiple comparison correction. From this peak-vertex, each participant's relative power is plotted (left) separately for the EC (magenta) and EO (green) conditions and connected with gray lines. The box plots illustrate the mean, first and third quartiles, and the whiskers indicate the minima and maxima. The violin plots illustrate the probability density. Each peak-vertex was labeled with the Harvard-Oxford cortical atlas. Relative alpha power was stronger in EC compared to EO condition, with differences mostly confined to posterior cortices and peaking in the occipital.

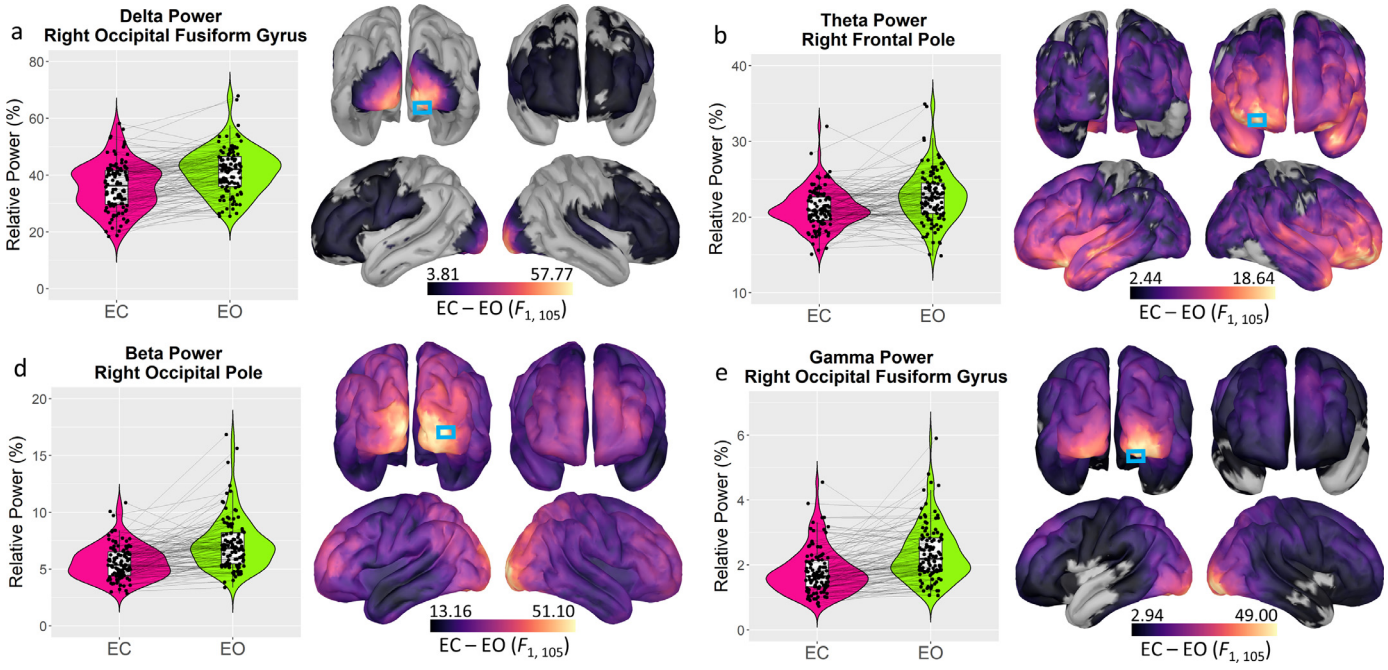

Fig. 2. Differences in resting state spontaneous activity in EC relative to EO. Cortical surface maps display the vertex-wise F-values representing the comparison of EC to EO relative power passing a TFCE threshold, with the blue box indicating the vertex containing the largest difference. The boxplots illustrate the individual data points from the vertex showing the strongest condition effect following multiple comparison correction. From this peak-vertex, each participant's relative power is plotted to the left of the corresponding cortical surface map separately for the EC (magenta) and EO (green) conditions and connected with gray lines. The box plots illustrate the mean, first and third quartiles, and the whiskers indicate the minima and maxima. The violin plots illustrate the probability density. For each canonical frequency band, the EC compared to EO differences were largely concentrated in the occipital cortices. (A) Relative delta differences included occipital and frontal cortices and were stronger in the EO condition. (B) Theta differences extended over much of the brain, excluding the sensorimotor strip, and were stronger in the EO condition. Relative power was stronger in the EO compared to EC condition and extended across most of the brain in the beta (C) and gamma (D) spectral ranges. Scale bars are shown beneath each set of maps.

Table 1
Demographic characteristics of the final sample.

	Male	Female	p-Value
Age range (years)	9.03–14.85	9.34–15.20	-
Mean age (years)	12.01	11.79	0.48
Race (White/Black or African American/Other/Unknown)	47/1/2/3	42/3/7/3	0.26
Ethnicity (Not Hispanic or Latino/Hispanic or Latino/Unknown)	48/5/0	50/4/1	0.57
Handedness (R/L/both)	49/3/1	53/2/0	0.52

Note: Differences in mean age between males and females were assessed using an independent samples *t*-test; differences in race, ethnicity, and handedness were assessed using chi-square tests.

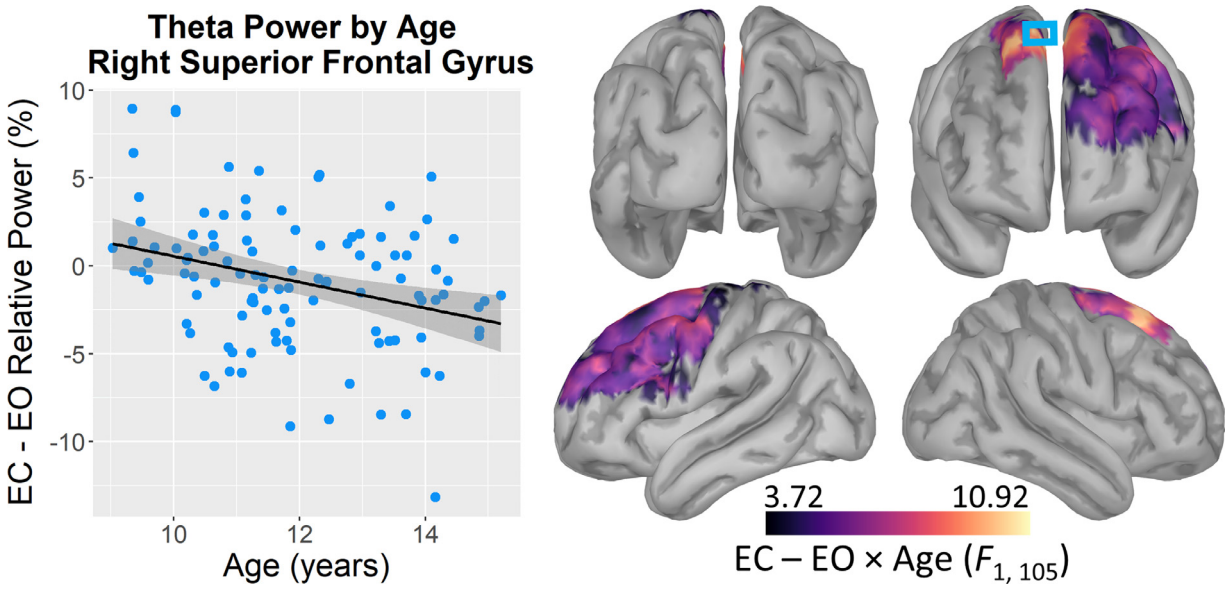

Fig. 3. Developmental differences in the relationship between EC – EO conditions. Cortical surface maps (right) display the vertex-wise F-values representing the relationship between EC and EO relative power as a function of age. The blue box denotes the vertex containing the strongest relationship. The scatter plot is for illustration only and shows data from the vertex with the strongest effect of age following multiple comparison correction. From this vertex, the EC – EO relative power is plotted (left; y-axis) against age (x-axis) across all participants. The least squares line is plotted in black, and the shaded region illustrates the 95% confidence interval. Older adolescents exhibited stronger theta power in the EO compared to EC condition in bilateral frontal cortical clusters, although the effect was much more widespread in the left hemisphere.

frontal pole ($F_{1, 105}$ = 18.64, p < .001). In the beta-band (Fig. 2), this difference was observed across the entire brain, with a peak difference located in the right occipital pole ($F_{1, 105}$ = 51.10, p < .001). Lastly, differences in the gamma-band (Fig. 2) were observed in two bilateral clusters spanning the occipital, parietal, temporal, and frontal lobes, with a peak difference in the right occipital fusiform gyrus ($F_{1, 105}$ = 49.00, p < .001).

To determine if these differences in the distribution of power amongst the canonical bands (i.e., relative power) also translated to greater total absolute power, we probed the total power in each condition and found that it was stronger in the EC relative to EO condition (see supplemental section S2). Thus, in interpreting these results, it should be emphasized that our key findings reflect that the distribution of overall power differs between conditions, with the EC condition having a much higher percent of its total power in the alpha band and the EO condition having a much higher percent of its total power in the other bands.

3.3. Developmental differences in eyes-open versus - closed resting activity

Conditional power differences (EC–EO) with age, controlling for sex, were detected in the theta frequency band (Fig. 3). The youngest participants exhibited stronger theta in EC relative EO, which decreased in older participants and eventually reversed (i.e., EO > EC) in two separate clusters, including a smaller right frontal cluster and a large left frontal cluster, with a peak difference located in the right superior frontal gyrus ($F_{1, 105}$ = 10.92, p < 0.01).

3.3. Sex differences in eyes-open versus - closed resting state activity

Next, we tested for conditional power differences (EC–EO) by sex, controlling for age, but no differences survived multiple comparisons correction in any of the frequency bands.

4. Discussion

In the current study, we examined differences in spontaneous cortical activity between EO versus EC resting-state paradigms in a large sample of children and adolescents (9–15 years). We found that relative alpha power was stronger in EC compared to EO, especially in the occipital cortices. Conversely, the relative power in the other frequency bands (i.e., delta, theta, beta, and gamma) was stronger during the EO relative to EC condition, with these differences also prominently concentrated in the occipital cortex for delta, while being much more widespread for the other frequency bands. In addition, we assessed developmental differences in these conditional effects, which revealed that the increased theta power in the EO relative to EC condition tends to strengthen (i.e., becomes stronger in the EO condition) as individuals approach young adulthood, especially in the superior frontal gyri.

Consistent with our hypothesis and previous work, the relative power differences between EC and EO conditions included visual re-

gions in the occipital cortices in all cases. The stronger relative alpha power in EC compared to EO rest, peaking in the occipital pole but extending across the entire occipital lobe, is consistent with the classical alpha effect whereby stronger alpha power is indicative of an idling visual cortex (Pfurtscheller, 1992) and/or reduced processing of external visual sensory information (Klimesch et al., 2007). Along these lines, increased occipital beta and gamma power, indicative of increased cortical processing (Hoogenboom et al., 2006; Ray and Cole, 1985), was observed in EO compared to EC conditions. These results suggest that EO compared to EC rest involves a general increase in visual cortical activity, presumably due to the presence of visual information.

Interestingly, delta and theta also showed increased relative power during EO compared to EC rest. The difference in theta activity covered a large portion of the brain, including a peak difference in the parietal cortex and local peaks in the occipital and frontal cortices. This effect is consistent with previous work linking theta activity to a variety of cognitive (Nigbur et al., 2011; Cavanagh and Frank, 2014) and attentional (Kawasaki and Yamaguchi, 2012; Torrence et al., 2021) processes, involving both frontal and posterior cortical regions (Knyazev, 2007), including the periodic sampling of unattended visual information (Spyropoulos et al., 2018; Fiebelkorn and Kastner, 2019) and, more generally, navigation of the sensory environment (Clarke, et al., 2018; Begus et al., 2015; Orekhova et al., 2006). Similarly, increased delta activity in posterior regions has been related to the detection of salient information (Knyazev, 2012; Harmony, 2013; Olde Dubbelink et al., 2008) and in promoting motivated behavior (Knyazev, 2007). In the context of the current results, the increased relative delta power during EO is likely related to the presence of visual information. Taken together, increases in theta and delta relative power, as with the findings in the faster frequencies, suggest that the EO resting state more strongly engages brain processes related to the processing of visual sensory information.

The developmental differences we observed were limited to the theta frequency band. While the conditional difference between EC and EO for theta was most prominent in the frontal pole, the effects also extended across many other areas including temporal and occipital cortices and the developmental differences were concentrated in the medial frontal cortex. Importantly, the difference in total absolute power between EC and EO conditions was not related to age, suggesting that this relationship between age and relative theta power can likely be more broadly interpreted. The location of this age-related difference is consistent with earlier findings showing that higher tier, association regions undergo structural development that extends relatively later than the early developing low-level sensory regions (Gogtay et al., 2004; Wierenga et al., 2014). These age-related theta differences likely reflect the maturation of frontal regions involved in attention processes (Kastner et al., 1999; Scolari et al., 2015), which have been linked to frontal theta activity (Kam et al., 2018). Indeed, frontal theta has been implicated as a marker of cognitive control processes (Cavanagh and Frank, 2014) during increased attention demands (Magosso et al., 2021, Sauseng et al., 2007). To summarize, the developmental changes observed here in theta spontaneous cortical activity may reflect underlying functional development of brain regions involved in higher-order attention processes as these children enter adolescence and progress toward early adulthood.

More broadly, the current results are drawn from a large sample of typically developing youth and thus contribute to establishing a baseline for the development of spontaneous cortical activity that may hold relevance in understanding neurodevelopmental disorders such as attention-deficit hyperactive disorder (ADHD; Barry et al., 2003; Clarke et al., 2020), a disorder characterized by inattentiveness and impulsivity (American Psychiatric Association, 2000). The limited number of studies using fMRI and EEG that have directly compared EC to EO conditions have found that individuals with ADHD show a smaller difference between EC and EO alpha power (Loo et al., 2010; Fonseca et al., 2013; but see Bellato et al. 2020) as well as theta power (Buyk and Wiersema, 2014; Woltering et al., 2012). Given that our developmental differences in EC compared to EO spontaneous cortical activity appear to implicate visual attention processes, including frequency bands outside the alpha range, future research should explore the extent to which EC compared to EO differences may be used to identify early markers of ADHD.

Finally, care should be taken to interpret the data in the context of the specific analysis that we performed. Notably, the current results represent the difference between EC and EO conditions in *normalized* spectral units, where each frequency band is quantified as a percentage of the total spectral power, consistent with several previous reports (Candelaria-Cook et al., 2022; Lew et al., 2021; Niso et al., 2019; Ott et al., 2021; Wiesman et al., 2021, but see Muthuraman et al. 2015 who compared absolute power). Given that the total absolute power was greater in the EC compared to EO condition, it is possible that the stronger *relative* delta, theta, beta, and gamma power in the EO condition could instead show that the distribution of *absolute* power among the canonical bands differed between the conditions, with alpha having a much larger share of the overall absolute power in the EC relative to the EO condition. While outside the scope of the current report, future work should explore whether differences in EC and EO conditions are affected by the use of absolute versus relative power. Along these lines, differences in total power may be driven by the 1/frequency slope of the spectrum (i.e., the aperiodic activity; Gerster et al., 2022; Miller et al., 2009). In this regard, resting condition differences in aperiodic activity have not been widely explored and to date have yielded mixed results (Demru and Fraschini, 2020; Hill et al., 2022) and thus should be subject to future investigation.

Before closing, it is important to note several limitations which may be addressed in future studies. First, this study implemented a cross-sectional design; the developmental changes observed in the current study should be tested in the future using a longitudinal design to draw stronger conclusions. Similarly, future work should determine whether the developmental differences observed here are related to specific pubertal stages. This could be done by implementing the Sexual Maturation Scale (Morris and Udry, 1980), Pubertal Development Scale (Petersen et al., 1988), and/or measuring hormones directly to assess pubertal status and how it relates to differences in EO versus EC rest. Further, the current sample contains somewhat restricted demographics, particularly with respect to race and ethnicity, which may limit the generalizability of the findings. Importantly, while the resting design possesses many strengths, as discussed in the introduction, it also limits the interpretation of some of the functional differences observed in this and other studies. Therefore, future work should directly test whether the developmental differences in spontaneous cortical activity may explain differences in task-based neural responses. Lastly, no measure was taken to assess drowsiness/sleep states during the periods of rest. Given that early stages of sleep are associated with a smaller alpha/theta ratio across the cortex (Rechtschaffen and Kales, 1968), future work should determine if any resting condition differences between EC and EO are related to differences in sleep states.

To summarize, the current study found increases in delta, theta, beta, and gamma relative power during EO relative to EC, along with a decrease in relative alpha power; these differences were generally strongest in posterior regions including the occipital cortex, but also extended anteriorly to include broad regions of the brain. These results are consistent with previous studies whereby differences between EC and EO involved visual sensory regions. The developmental changes observed in alpha and beta were centered on later developing brain regions, including those involved in higher cognitive processes such as attention. Overall, these results suggest that collapsing resting state findings across studies that used different paradigms (e.g., EO versus EC) should be done with caution and in many cases there are benefits to treating these conditions as separate “tasks.” In fact, future studies should strategically choose EO or EC depending on the study goals (e.g., accentuate brain activity in visual sensory regions). Future work may also benefit from exploring these resting state differences in the context of understanding developmental brain disorders such as ADHD.

Data and code availability statement

The data used in this article will be made publicly available through the COINS framework at the completion of the study (https://coins.trendscenter.org/). Data processing pipelines followed previous studies (Niso et al., 2019) using a combination of Brainstorm (Tadel et al., 2011), which is documented and freely available for download online under the GNU general public license (http://neuroimage.usc.edu/brainstorm), and CAT12 (Gaser and Dahnke, 2016) toolboxes.

Funding

This work was supported by the National Science Foundation (#1539067 to TWW, YPW, JMS, and VDC and #2112455 to VDC), the National Institutes of Health (R01-MH121101, R01-MH116782, R01-MH118013, and P20-GM144641 to TWW; R01-EB020407, R01-MH118695, and R01-MH123610 to VDC; R56-MH124925 to YPW). Funding agencies had no part in the study design or the writing of this report.

Declaration of Competing Interest

All authors report no biomedical financial interests or potential conflicts of interest.

Credit authorship contribution statement

Nathan M. Petro: Formal analysis, Software, Visualization, Writing – original draft, Writing – review & editing. **Lauren R. Ott:** Formal analysis, Writing – review & editing. **Samantha H. Penhale:** Formal analysis, Writing – review & editing. **Maggie P. Rempe:** Formal analysis, Writing – review & editing. **Christine M. Embury:** Writing – review & editing. **Giorgia Picci:** Writing – review & editing. **Yu-Ping Wang:** Conceptualization, Methodology, Writing – review & editing. **Julia M. Stephen:** Conceptualization, Methodology, Writing – review & editing. **Vince D. Calhoun:** Conceptualization, Methodology, Writing – review & editing. **Tony W. Wilson:** Conceptualization, Methodology, Supervision, Writing – review & editing.

Acknowledgments

The authors wish to thank the volunteers for participating in this study, as well as all research staff and local collaborators for their contributions to this work. The authors wish to specifically thank Nichole Knott for extensive help with the MEG recordings.

Supplementary materials

Supplementary material associated with this article can be found, in the online version, at doi:10.1016/j.neuroimage.2022.119337.

References

Adrian, E.D., 1944. Brain rhythms. Nature 153 (3882), 360–362. doi:10.1038/153360a0.
Agcaoglu, O., Wilson, T.W., Wang, Y.P., Stephen, J.M., Calhoun, V.D., 2020. Dynamic resting-state connectivity differences in eyes open versus eyes closed conditions. Brain Connect. doi:10.1089/brain.2020.0768.
Allen, E.A., Damaraju, E., Eichele, T., Wu, L., Calhoun, V.D., 2018. EEG signatures of dynamic functional network connectivity states. Brain Topogr. 31 (1), 101–116. doi:10.1007/s10548-017-0546-2.
American Psychiatric Association, 2000. Diagnostic and Statistical Manual of Mental Disorders, 4. APA, Washington, DC.
Ashburner, J., Friston, K.J., 2005. Unified segmentation. Neuroimage 26 (3), 839–851. doi:10.1016/j.neuroimage.2005.02.018.
Azeez, A.K., Biswal, B.B., 2017. A review of resting-state analysis methods. Neuroimaging Clin. N. Am. 27 (4), 581–592. doi:10.1016/j.nic.2017.06.001.
Baillet, S., 2017. Magnetoencephalography for brain electrophysiology and imaging. Nat. Neurosci. 20 (3), 327–339. doi:10.1038/nn.4504.
Barry, R.J., Clarke, A.R., Johnstone, S.J., 2003. A review of electrophysiology in attention-deficit/hyperactivity disorder: i. qualitative and quantitative electroencephalography. Clin. Neurophysiol. 114 (2), 171–183. doi:10.1016/S1388-2457(02)00362-0.
Barry, R.J., Clarke, A.R., Johnstone, S.J., Brown, C.R., 2009. EEG differences in children between eyes-closed and eyes-open resting conditions. Clin. Neurophysiol. 120 (10), 1806–1811. doi:10.1016/j.clinph.2009.08.006.
Barry, R.J., Clarke, A.R., Johnstone, S.J., Magee, C.A., Rushby, J.A., 2007. EEG differences between eyes-closed and eyes-open resting conditions. Clin. Neurophysiol. 118 (12), 2765–2773. doi:10.1016/j.clinph.2007.07.028.
Barry, R., Rushby, J., Wallace, M., Clarke, A., Johnstone, S., Zlojutro, I., 2005. Caffeine effects on resting-state arousal. Clin. Neurophysiol. 116 (11), 2693–2700. doi:10.1016/j.clinph.2005.08.008.
Begus, K., Southgate, V., Gliga, T., 2015. Neural mechanisms of infant learning: differences in frontal theta activity during object exploration modulate subsequent object recognition. Biol. Lett. 11 (5), 20150041. doi:10.1098/rsbl.2015.0041.
Bellato, A., Arora, I., Kochhar, P., Hollis, C., Groom, M.J., 2020. Atypical electrophysiological indices of eyes-open and eyes-closed resting-state in children and adolescents with ADHD and autism. Brain Sci. 10 (5), 272. doi:10.3390/brainsci10050272.
Berger, H., 1929. Über das elektroenkephalogramm des menschen. Arch. Psychiatrie Nervenkrankh. 87 (1), 527–570.
Biswal, B., Zerrin Yetkin, F., Haughton, V.M., Hyde, J.S., 1995. Functional connectivity in the motor cortex of resting human brain using echo-planar mri. Magn. Reson. Med. 34 (4), 537–541. doi:10.1002/mrm.1910340409.
Buyck, I., Wiersema, J.R., 2014. State-related electroencephalographic deviances in attention deficit hyperactivity disorder. Res. Dev. Disabil. 35 (12), 3217–3225. doi:10.1016/j.ridd.2014.08.003.
Candelaria-Cook, F.T., Solis, I., Schendel, M.E., Wang, Y.P., Wilson, T.W., Calhoun, V.D., Stephen, J.M., 2022. Developmental trajectory of MEG resting-state oscillatory activity in children and adolescents: a longitudinal reliability study. Cereb. Cortex doi:10.1093/cercor/bhac023, bhac023.
Cavanagh, J.F., Frank, M.J., 2014. Frontal theta as a mechanism for cognitive control. Trends Cogn. Sci. 18 (8), 414–421. doi:10.1016/j.tics.2014.04.012.
Clarke, A.R., Barry, R.J., Johnstone, S., 2020. Resting state EEG power research in attention-deficit/hyperactivity disorder: a review update. Clin. Neurophysiol. 131 (7), 1463–1479. doi:10.1016/j.clinph.2020.03.029.
Clarke, A., Roberts, B.M., Ranganath, C., 2018. Neural oscillations during conditional associative learning. Neuroimage 174, 485–493. doi:10.1016/j.neuroimage.2018.03.053.
Cohen, D., 1968. Magnetoencephalography: evidence of magnetic fields produced by alpha-rhythm currents. Science 161 (3843), 784–786. doi:10.1126/science.161.3843.784.
Demuru, M., Fraschini, M., 2020. EEG fingerprinting: subject-specific signature based on the aperiodic component of power spectrum. Comput. Biol. Med. 120, 103748. doi:10.1016/j.compbiomed.2020.103748.
Drysdale, A.T., Grosenick, L., Downar, J., Dunlop, K., Mansouri, F., Meng, Y., Fetcho, R.N., Zebley, B., Oathes, D.J., Etkin, A., Schatzberg, A.F., Sudheimer, K., Keller, J., Mayberg, H.S., Gunning, F.M., Alexopoulos, G.S., Fox, M.D., Pascual-Leone, A., Voss, H.U., Liston, C., 2017. Resting-state connectivity biomarkers define neurophysiological subtypes of depression. Nat. Med. 23 (1), 28–38. doi:10.1038/nm.4246.
Ergenoglu, T., Demiralp, T., Bayraktaroglu, Z., Ergen, M., Beydagi, H., Uresin, Y., 2004. Alpha rhythm of the EEG modulates visual detection performance in humans. Cognit. Brain Res. 20 (3), 376–383. doi:10.1016/j.cogbrainres.2004.03.009.
Fiebelkorn, I.C., Kastner, S., 2019. A rhythmic theory of attention. Trends Cogn. Sci. 23 (2), 87–101. doi:10.1016/j.tics.2018.11.009.
Fonov, V., Evans, A., McKinstry, R., Almli, C., Collins, D., 2009. Unbiased nonlinear average age-appropriate brain templates from birth to adulthood. Neuroimage 47, S102. doi:10.1016/S1053-8119(09)70884-5.
Fonseca, L.C., Tedrus, G.M.A.S., Bianchini, M.C., Silva, T.F., 2013. Electroencephalographic alpha reactivity on opening the eyes in children with attention-deficit hyperactivity disorder. Clin. EEG Neurosci. 44 (1), 53–57. doi:10.1177/1550059412445659.
Fox, M.D., Raichle, M.E., 2007. Spontaneous fluctuations in brain activity observed with functional magnetic resonance imaging. Nat. Rev. Neurosci. 8 (9), 700–711. doi:10.1038/nrn2201.
Gaser, C., & Dahnke, R. (2016). *CAT - a computational anatomy toolbox for the analysis of structural MRI data*. HBM 2016, 336–348.
Gerster, M., Waterstraat, G., Litvak, V., Lehnertz, K., Schnitzler, A., Florin, E., Curio, G., Nikulin, V., 2022. Separating neural oscillations from aperiodic 1/f activity: challenges and recommendations. Neuroinformatics doi:10.1007/s12021-022-09581-8.
Goddings, A.L., Beltz, A., Peper, J.S., Crone, E.A., Braams, B.R., 2019. Understanding the role of puberty in structural and functional development of the adolescent brain. J. Res. Adolesc. 29 (1), 32–53. doi:10.1111/jora.12408.
Gogtay, N., Giedd, J.N., Lusk, L., Hayashi, K.M., Greenstein, D., Vaituzis, A.C., Nugent, T.F., Herman, D.H., Clasen, L.S., Toga, A.W., Rapoport, J.L., Thompson, P.M., 2004. Dynamic mapping of human cortical development during childhood through early adulthood. Proc. Natl. Acad. Sci. 101 (21), 8174–8179. doi:10.1073/pnas.0402680101.
Gómez, C., M Pérez-Macías, J., Poza, J., Fernández, A., Hornero, R., 2013. Spectral changes in spontaneous MEG activity across the lifespan. J. Neural Eng. 10 (6), 066006. doi:10.1088/1741-2560/10/6/066006.
Harmony, T., 2013. The functional significance of delta oscillations in cognitive processing. Front. Integr. Neurosci. 7. doi:10.3389/fnint.2013.00083.
Hill, A.T., Clark, G.M., Bigelow, F.J., Lum, J.A.G., Enticott, P.G., 2022. Periodic and aperiodic neural activity displays age-dependent changes across early-to-middle childhood. Dev. Cogn. Neurosci. 54, 101076. doi:10.1016/j.dcn.2022.101076.

Hoogenboom, N., Schoffelen, J.M., Oostenveld, R., Parkes, L.M., Fries, P., 2006. Localizing human visual gamma-band activity in frequency, time and space. Neuroimage 29 (3), 764–773. doi:10.1016/j.neuroimage.2005.08.043.

Hoshi, H., Shigihara, Y., 2020. Age- and gender-specific characteristics of the resting-state brain activity: a magnetoencephalography study. Aging 12 (21), 21613–21637. doi:10.18632/aging.103956.

Huang, M.X., Mosher, J.C., Leahy, R.M., 1999. A sensor-weighted overlapping-sphere head model and exhaustive head model comparison for MEG. Phys. Med. Biol. 44 (2), 423–440. doi:10.1088/0031-9155/44/2/010.

Hunt, B.A.E., Wong, S.M., Vandewouw, M.M., Brookes, M.J., Dunkley, B.T., Taylor, M.J., 2019. Spatial and spectral trajectories in typical neurodevelopment from childhood to middle age. Netw. Neurosci. 3 (2), 497–520. doi:10.1162/netn_a_00077.

Ille, N., Berg, P., Scherg, M., 2002. Artifact correction of the ongoing EEG using spatial filters based on artifact and brain signal topographies. J. Clin. Neurophysiol. 19 (2), 113–124. doi:10.1097/00004691-200203000-00002.

Kam, J.W.Y., Solbakk, A.K., Endestad, T., Meling, T.R., Knight, R.T., 2018. Lateral prefrontal cortex lesion impairs regulation of internally and externally directed attention. Neuroimage 175, 91–99. doi:10.1016/j.neuroimage.2018.03.063.

Kastner, S., Pinsk, M.A., De Weerd, P., Desimone, R., Ungerleider, L.G., 1999. Increased activity in human visual cortex during directed attention in the absence of visual stimulation. Neuron 22 (4), 751–761. doi:10.1016/S0896-6273(00)80734-5.

Kawasaki, M., Yamaguchi, Y., 2012. Effects of subjective preference of colors on attention-related occipital theta oscillations. Neuroimage 59 (1), 808–814. doi:10.1016/j.neuroimage.2011.07.042.

Klimesch, W., Sauseng, P., Hanslmayr, S., 2007. EEG alpha oscillations: The inhibition–timing hypothesis. Brain Res. Rev. 53 (1), 63–88. doi:10.1016/j.brainresrev.2006.06.003.

Knyazev, G.G., 2007. Motivation, emotion, and their inhibitory control mirrored in brain oscillations. Neurosci. Biobehav. Rev. 31 (3), 377–395. doi:10.1016/j.neubiorev.2006.10.004.

Knyazev, G.G., 2012. EEG delta oscillations as a correlate of basic homeostatic and motivational processes. Neurosci. Biobehav. Rev. 36 (1), 677–695. doi:10.1016/j.neubiorev.2011.10.002.

Lew, B.J., Fitzgerald, E.E., Ott, L.R., Penhale, S.H., Wilson, T.W., 2021. Three-year reliability of MEG resting-state oscillatory power. Neuroimage 243, 118516. doi:10.1016/j.neuroimage.2021.118516.

Loo, S.K., Hale, T.S., Hanada, G., Macion, J., Shrestha, A., McGough, J.J., McCracken, J.T., Nelson, S., Smalley, S.L., 2010. Familial clustering and DRD4 effects on electroencephalogram measures in multiplex families with attention deficit/hyperactivity disorder. J. Am. Acad. Child Adolesc. Psychiatry 49 (4), 368–377. doi:10.1016/j.jaac.2010.01.002.

Magosso, E., Ricci, G., Ursino, M., 2021. Alpha and theta mechanisms operating in internal-external attention competition. J. Integr. Neurosci. 20 (1), 1. doi:10.31083/j.jin.2021.01.422.

Manjón, J.V., Coupé, P., Martí-Bonmatí, L., Collins, D.L., Robles, M., 2010. Adaptive non-local means denoising of MR images with spatially varying noise levels. J. Magn. Reson. Imaging 31 (1), 192–203. doi:10.1002/jmri.22003.

Marusak, H.A., Calhoun, V.D., Brown, S., Crespo, L.M., Sala-Hamrick, K., Gotlib, I.H., Thomason, M.E., 2017. Dynamic functional connectivity of neurocognitive networks in children. Hum. Brain Mapp. 38 (1), 97–108. doi:10.1002/hbm.23346.

Michels, L., Muthuraman, M., Lüchinger, R., Martin, E., Anwar, A.R., Raethjen, J., Brandeis, D., Siniatchkin, M., 2013. Developmental changes of functional and directed resting-state connectivities associated with neuronal oscillations in EEG. Neuroimage 81, 231–242. doi:10.1016/j.neuroimage.2013.04.030.

Miller, K.J., Sorensen, L.B., Ojemann, J.G., den Nijs, M., 2009. Power-law scaling in the brain surface electric potential. PLoS Comput. Biol. 5 (12), e1000609. doi:10.1371/journal.pcbi.1000609.

Mills, K.L., Tamnes, C.K., 2014. Methods and considerations for longitudinal structural brain imaging analysis across development. Dev. Cogn. Neurosci. 9, 172–190. doi:10.1016/j.dcn.2014.04.004.

Morris, N.M., Udry, J.R., 1980. Validation of a self-administered instrument to assess stage of adolescent development. J. Youth Adolesc. 9 (3), 271–280. doi:10.1007/BF02088471.

Muthuraman, M., Moliadze, V., Mideksa, K.G., Anwar, A.R., Stephani, U., Deuschl, G., Freitag, C.M., Siniatchkin, M., 2015. EEG-MEG Integration Enhances the Characterization of Functional and Effective Connectivity in the Resting State Network. PLoS ONE 10, e0140832. doi: 10.1371/journal.pone.0140832.

Nigbur, R., Ivanova, G., Stürmer, B., 2011. Theta power as a marker for cognitive interference. Clin. Neurophysiol. 122 (11), 2185–2194. doi:10.1016/j.clinph.2011.03.030.

Niso, G., Tadel, F., Bock, E., Cousineau, M., Santos, A., Baillet, S., 2019. Brainstorm pipeline analysis of resting-state data from the open MEG archive. Front. Neurosci. 13, 284. doi:10.3389/fnins.2019.00284.

Olde Dubbelink, K.T.E., Felius, A., Verbunt, J.P.A., van Dijk, B.W., Berendse, H.W., Stam, C.J., Delemarre-van de Waal, H.A., 2008. Increased resting-state functional connectivity in obese adolescents; a magnetoencephalographic pilot study. PLoS One 3 (7), e2827. doi:10.1371/journal.pone.0002827.

Orekhova, E., Stroganova, T., Posikera, I., Elam, M., 2006. EEG theta rhythm in infants and preschool children. Clin. Neurophysiol. 117 (5), 1047–1062. doi:10.1016/j.clinph.2005.12.027.

Ott, L.R., Penhale, S.H., Taylor, B.K., Lew, B.J., Wang, Y.-P., Calhoun, V.D., Stephen, J.M., Wilson, T.W., 2021. Spontaneous cortical MEG activity undergoes unique age- and sex-related changes during the transition to adolescence. Neuroimage 244, 118552. doi:10.1016/j.neuroimage.2021.118552.

Patriat, R., Molloy, E.K., Meier, T.B., Kirk, G.R., Nair, V.A., Meyerand, M.E., Prabhakaran, V., Birn, R.M., 2013. The effect of resting condition on resting-state fMRI reliability and consistency: a comparison between resting with eyes open, closed, and fixated. Neuroimage 78, 463–473. doi:10.1016/j.neuroimage.2013.04.013.

Petersen, A.C., Crockett, L., Richards, M., Boxer, A., 1988. A self-report measure of pubertal status: reliability, validity, and initial norms. J. Youth Adolesc. 17 (2), 117–133. doi:10.1007/BF01537962.

Pfurtscheller, G., 1992. Event-related synchronization (ERS): An electrophysiological correlate of cortical areas at rest. Electroencephalogr. Clin. Neurophysiol. 83 (1), 62–69. doi:10.1016/0013-4694(92)90133-3.

Rajapakse, J.C., Giedd, J.N., Rapoport, J.L., 1997. Statistical approach to segmentation of single-channel cerebral MR images. IEEE Trans. Med. Imaging 16 (2), 176–186. doi:10.1109/42.563663.

Ray, W.J., Cole, H.W., 1985. EEG alpha activity reflects attentional demands, and beta activity reflects emotional and cognitive processes. Science 228 (4700), 750–752 (*New York, N.Y.)*.

Rechtschaffen, A., & Kales, A. (1968). *A manual of standardized terminology, techniques and scoring system for sleep stages of human subjects*. Los Angeles, UCLA Brain Information Service/Brain Research Institute, 1968.

Sauseng, P., Hoppe, J., Klimesch, W., Gerloff, C., Hummel, F.C., 2007. Dissociation of sustained attention from central executive functions: Local activity and interregional connectivity in the theta range. Eur. J. Neurosci. 25 (2), 587–593. doi:10.1111/j.1460-9568.2006.05286.x.

Scolari, M., Seidl-Rathkopf, K.N., Kastner, S., 2015. Functions of the human frontoparietal attention network: evidence from neuroimaging. Curr. Opin. Behav. Sci. 1, 32–39. doi:10.1016/j.cobeha.2014.08.003.

Segalowitz, S.J., Santesso, D.L., Jetha, M.K., 2010. Electrophysiological changes during adolescence: a review. Brain Cogn. 72 (1), 86–100. doi:10.1016/j.bandc.2009.10.003.

Smith, S., Nichols, T., 2009. Threshold-free cluster enhancement: addressing problems of smoothing, threshold dependence and localisation in cluster inference. Neuroimage 44 (1), 83–98. doi:10.1016/j.neuroimage.2008.03.061.

Spyropoulos, G., Bosman, C.A., Fries, P., 2018. A theta rhythm in macaque visual cortex and its attentional modulation. Proc. Natl. Acad. Sci. 115 (24), E5614–E5623. doi:10.1073/pnas.1719433115.

Tadel, F., Baillet, S., Mosher, J. C., Pantazis, D., Leahy, R. M., 2011. Brainstorm: A User-Friendly Application for MEG/EEG Analysis. Computational Intelligence and Neuroscience 2011, 1–13. doi:10.1155/2011/879716.

Tadel, F., Bock, E., Niso, G., Mosher, J.C., Cousineau, M., Pantazis, D., Leahy, R.M., Baillet, S., 2019. MEG/EEG group analysis with brainstorm. Front. Neurosci. 13, 76. doi:10.3389/fnins.2019.00076.

Taulu, S., Simola, J., 2006. Spatiotemporal signal space separation method for rejecting nearby interference in MEG measurements. Phys. Med. Biol. 51 (7), 1759–1768. doi:10.1088/0031-9155/51/7/008.

Torrence, R.D., Troup, L.J., Rojas, D.C., Carlson, J.M., 2021. Enhanced contralateral theta oscillations and N170 amplitudes in occipitotemporal scalp regions underlie attentional bias to fearful faces. Int. J. Psychophysiol. 165, 84–91. doi:10.1016/j.ijpsycho.2021.04.002.

Uddin, L.Q., Supekar, K.S., Ryali, S., Menon, V., 2011. Dynamic reconfiguration of structural and functional connectivity across core neurocognitive brain networks with development. J. Neurosci. 31 (50), 18578–18589. doi:10.1523/JNEUROSCI.4465-11.2011.

Uhlhaas, P.J., Roux, F., Rodriguez, E., Rotarska-Jagiela, A., Singer, W., 2010. Neural synchrony and the development of cortical networks. Trends Cogn. Sci. 14 (2), 72–80. doi:10.1016/j.tics.2009.12.002.

Uusitalo, M.A., Ilmoniemi, R.J., 1997. Signal-space projection method for separating MEG or EEG into components. Med. Biol. Eng. Comput. 35 (2), 135–140. doi:10.1007/BF02534144.

Van Dijk, K.R.A., Hedden, T., Venkataraman, A., Evans, K.C., Lazar, S.W., Buckner, R.L., 2010. Intrinsic functional connectivity as a tool for human connectomics: theory, properties, and optimization. J. Neurophysiol. 103 (1), 297–321. doi:10.1152/jn.00783.2009.

Welch, P., 1967. The use of fast Fourier transform for the estimation of power spectra: a method based on time averaging over short, modified periodograms. IEEE Trans. Audio Electroacoust. 15 (2), 70–73. doi:10.1109/TAU.1967.1161901.

Wierenga, L.M., Langen, M., Oranje, B., Durston, S., 2014. Unique developmental trajectories of cortical thickness and surface area. Neuroimage 87, 120–126. doi:10.1016/j.neuroimage.2013.11.010.

Wiesman, A.I., da Silva Castanheira, J., Baillet, S., 2022. Stability of spectral estimates in resting-state magnetoencephalography: recommendations for minimal data duration with neuroanatomical specificity. Neuroimage 247, 118823. doi:10.1016/j.neuroimage.2021.118823.

Wiesman, A.I., Murman, D.L., Losh, R.A., Schantell, M., Christopher-Hayes, N.J., Johnson, H.J., Willett, M.P., Wolfson, S.L., Losh, K.L., Johnson, C.M., May, P.E., Wilson, T.W., 2022. Spatially resolved neural slowing predicts impairment and amyloid burden in Alzheimer's disease. Brain doi:10.1093/brain/awab430, awab430.

Wiesman, A.I., Murman, D.L., May, P.E., Schantell, M., Losh, R.A., Johnson, H.J., Willet, M.P., Eastman, J.A., Christopher-Hayes, N.J., Knott, N.L., Houseman, L.L., Wolfson, S.L., Losh, K.L., Johnson, C.M., Wilson, T.W., 2021. Spatio-spectral relationships between pathological neural dynamics and cognitive impairment along the Alzheimer's disease spectrum. Alzheimer's & Dementia: Diagnosis, Assessment & Disease Monitoring, 13(1) doi:10.1002/dad2.12200.

Wilson, T.W., Heinrichs-Graham, E., Proskovec, A.L., McDermott, T.J., 2016. Neuroimaging with magnetoencephalography: a dynamic view of brain pathophysiology. Transl. Res. 175, 17–36. doi:10.1016/j.trsl.2016.01.007.

Woltering, S., Jung, J., Liu, Z., Tannock, R., 2012. Resting state EEG oscillatory power differences in ADHD college students and their peers. Behav. Brain Funct. 8 (1), 60. doi:10.1186/1744-9081-8-60.